

Robustness Evaluation for ILQ Optimal Control Based on Inverse Reference Model (IRM) Hybrid Control of Single-phase Inverter Voltage/Current

K. A. Ahmadou and Hiroshi Takami

Shibaura Institute of Technology, Tokyo, Japan

Email: kaahmadou61@gmail.com, takami@sic.shibaura-it.ac.jp

Abstract—In this paper we propose a new control method that can follow dynamic reference inputs and has high robustness and gain. This control method is an easy process and analytically obtains optimal solution without trial and error. We also propose a new control method (hybrid control of voltage and current) in which output voltage control and current control of a single-phase inverter are combined into one control system. Several simulations were done using PSIM to verify the robustness of this new control method by changing the parameters such as resistance, capacitance and inductance.

Index Terms—ILQ optimal control, Reference model, single-phase inverter

I. INTRODUCTION

In order to help reduce environmental problems, the distribution of power generation controlled by single-phase inverter such as wind-power, solar power, fuel cell and micro gas turbine generation, becomes more and more significant [1]. In that case Phase Locked Loop (PLL) is commonly used to connect the inverter with utility power system. Connecting this device to the utility is very important to detect phase, amplitude and frequency for synchronizing the inverter [2,3]. However, the PLL detects them from sinusoidal waveform, so that we need strategy based on instantaneous control for a good sinusoidal characteristic, fast dynamic response and strong load adaptability.

The inverse Linear Quadratic (ILQ) method is practical servo- system on a basis of optimal control theory [4,5]. The ILQ system has many advantages such transfer function between inputs and outputs can be asymptotically designated for the desire specification, the optimal solutions are analytically obtained and their optimality are guaranteed and the optimal gains can be easily adjusted to obtain the desire responses at the point of use [6-8].

However, conventional ILQ control is type 1 which cannot follow the time-variant reference such as sinusoidal waveform. It is known that the type 2 or upper grade servo can follow it.

In this paper, we used the Hybrid control of single-phase inverter voltage and current combine into one control system.

II. METHOD AND SIMULATION

A. Method

1) Optimal control by inverse model

This model Fig. 1 has same number of inputs and outputs with measurable disturbance as shown (1) and (2):

$$\frac{d}{dt}x = Ax + Bu + Dd . \quad (1)$$

$$y = Cx . \quad (2)$$

If we denote a set of real vectors of order n , and a set of real matrices of order $n \times m$, then $x \in \mathbb{R}^n$:state variable, $u \in \mathbb{R}^m$: control input, $y \in \mathbb{R}^m$: output, d : disturbance. $A \in \mathbb{R}^{n \times n}$, $C \in \mathbb{R}^{m \times n}$, $D \in \mathbb{R}^{m \times l}$: represents a coefficient matrix .

Equations (1), (2) shall have the following properties:

- (1) It is controllable and observable.
- (2) Do not have a zero point at the origin.
- (3) Minimum phase system.

Since the minimum phase system has no instability zero, the inverse system of the stable minimum phase system is stable. Therefore, if the state variable obtained by inputting the target reference input to the stable inverse system and the control input are the ideal operating points, the following equation holds.

$$\frac{d}{dt}x_0 = Ax_0 + Bu_0 + Dd \quad (3)$$

$$y^* = Cx_0 \quad (4)$$

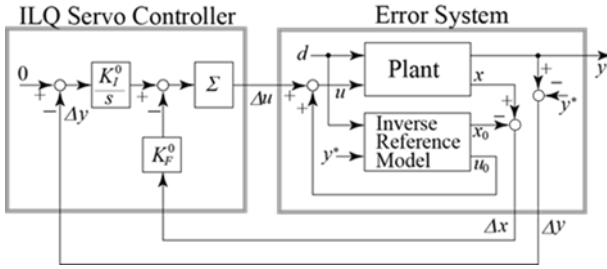


Figure 1. Configuration of the basic IMR (Inverse reference model)-ILQ servo system.

In fig.1 $K_F^0 \in \mathbb{R}^{m \times n}$, $K_I^0 \in \mathbb{R}^{m \times m}$ are reference optimal gain and $\Sigma \in \mathbb{R}^{m \times m}$ is gain adjustment parameter. The deviation between the plant of (1), (2) and (3), (4) gives the following deviation system (Error signal) as shown below:

$$\left. \begin{aligned} \Delta x &= x - x_0 \\ \Delta u &= u - u_0 \\ \Delta y &= y - y^* \end{aligned} \right\}. \quad (5)$$

$$\frac{d}{dt} \Delta x = A \Delta x + B \Delta u. \quad (6)$$

$$\Delta y = C \Delta x. \quad (7)$$

A new state variable is given by the following equation to derive the expansion system of the servo system:

$$\Delta z = z - z_0 = \frac{\Delta y}{s} \quad (8)$$

However, z_0 is the initial value of the integral of system.

Then, if the expansion state variable and the expansion system input are $x_e = [\Delta x^T \quad \Delta z^T]^T \in \mathbb{R} : [\quad]^T$ is the transposed equations from (6) to (8) for the following equations :

$$\frac{d}{dt} x_e = A_e x_e + B_e u_e. \quad (9)$$

Here, the coefficient matrix is given by the following equation:

$$A_e = \begin{bmatrix} A & 0 \\ C & 0 \end{bmatrix} \in \mathbb{R}^{(m+n) \times (m+n)}$$

$$B_e = \begin{bmatrix} B \\ 0 \end{bmatrix} \in \mathbb{R}^{(m+n) \times (m+n)}$$

On the other hand, from (8) and Fig. 1

$$u_e = -K_e x_e \quad (10)$$

$$K_e = \begin{bmatrix} \Sigma K_F^0 & \Sigma K_I^0 \end{bmatrix} \in \mathbb{R}^{(m+n) \times (m+n)}$$

Respectively. Therefore, the servo system in Fig. 1 is represented by a closed loop system with state feedback of (10) to the expansion plant of (9).

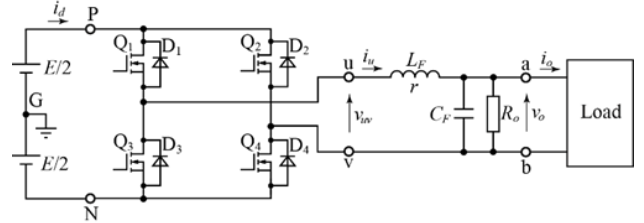


Figure 2. Single-phase Inverter Circuit.

B. Hybrid Control of Voltage and Current

Where, the terminal pair P-N is the DC input terminal of the inverter, the terminal pair u-v is an AC output terminal of the inverter, the terminal pair a-b is output terminal to the load. E is the DC supply voltage, i_d is the DC input current, v_{uv} and i_u are the voltage and current of the output terminal of the inverter, v_o and i_o are the voltage and current of the output (load). L_F , r and C_F are the inductance, winding resistance and capacitance of the LC low pass filter (LPF) for the inverter output voltage and the current, R_o is the output resistance. The parameters are shown in table 1.

C. Voltage Equation and State Equation in the single-phase inverter (Fig. 2)

The voltage equation is given by the following equation.

$$v_{uv} = L_F \frac{di_u}{dt} + r i_u + v_o \quad (11)$$

$$i_u = C_F \frac{dv_o}{dt} + \frac{v_o}{R_o} + i_o \quad (12)$$

$$\begin{aligned} \frac{d}{dt} \begin{bmatrix} v_o \\ i_u \end{bmatrix} &= \begin{bmatrix} -\frac{1}{R_o C_F} & \frac{1}{C_F} \\ -\frac{1}{L_F} & -\frac{r}{L_F} \end{bmatrix} \begin{bmatrix} v_o \\ i_u \end{bmatrix} + \begin{bmatrix} 0 \\ \frac{1}{L_F} \end{bmatrix} v_{uv} + \begin{bmatrix} -\frac{1}{C_F} \\ 0 \end{bmatrix} i_o \\ &= \begin{bmatrix} -1/T_C & 1/C_F \\ -1/L_F & -1/T_L \end{bmatrix} \begin{bmatrix} v_o \\ i_u \end{bmatrix} + \begin{bmatrix} 0 \\ 1/L_F \end{bmatrix} v_{uv} + \begin{bmatrix} -1/C_F \\ 0 \end{bmatrix} i_o \end{aligned} \quad (13)$$

Where $T_C = R_o C_F$ and $T_L = L_F / r$ are time constant.

Next when the current load i_o is flowing, the inverter is in a stable steady state and this is the operating point and the state equation is given by the following equation:

$$\frac{d}{dt} \begin{bmatrix} v_{o0} \\ i_{u0} \end{bmatrix} = \begin{bmatrix} -1/T_C & 1/C_F \\ -1/L_F & -1/T_L \end{bmatrix} \begin{bmatrix} v_{o0} \\ i_{u0} \end{bmatrix} + \begin{bmatrix} 0 \\ 1/L_F \end{bmatrix} v_{uv0} + \begin{bmatrix} -1/C_F \\ 0 \end{bmatrix} i_o \quad (14)$$

Then, the variation from the operating point is defined by the following equation.

$$\left. \begin{aligned} \Delta v_{uv} &= v_{uv} - v_{uv0} \\ \Delta i_u &= i_u - i_{u0} \\ \Delta v_o &= v_o - v_{o0} \end{aligned} \right\} \quad (15)$$

From the (13) to (15), we obtain the state equation for the deviation system of the following equation.

$$\frac{d}{dt} \begin{bmatrix} \Delta v_o \\ \Delta i_u \end{bmatrix} = \begin{bmatrix} -1/T_C & 1/C_F \\ -1/L_F & -1/T_L \end{bmatrix} \begin{bmatrix} \Delta v_o \\ \Delta i_u \end{bmatrix} + \begin{bmatrix} 0 \\ 1/L_F \end{bmatrix} \Delta v_{uv} \quad (16)$$

Therefore, the state variables, the control input and the coefficient matrix of the state equation of (6) are as follows.

State variable: $\Delta x = [\Delta v_o \ \Delta i_u]^T$

Control input: $\Delta u = \Delta v_{uv}$

Coefficient matrix: $A = \begin{bmatrix} -1/T_C & 1/C_F \\ -1/L_F & -1/T_L \end{bmatrix}$, $B = \begin{bmatrix} 0 \\ 1/L_F \end{bmatrix}$

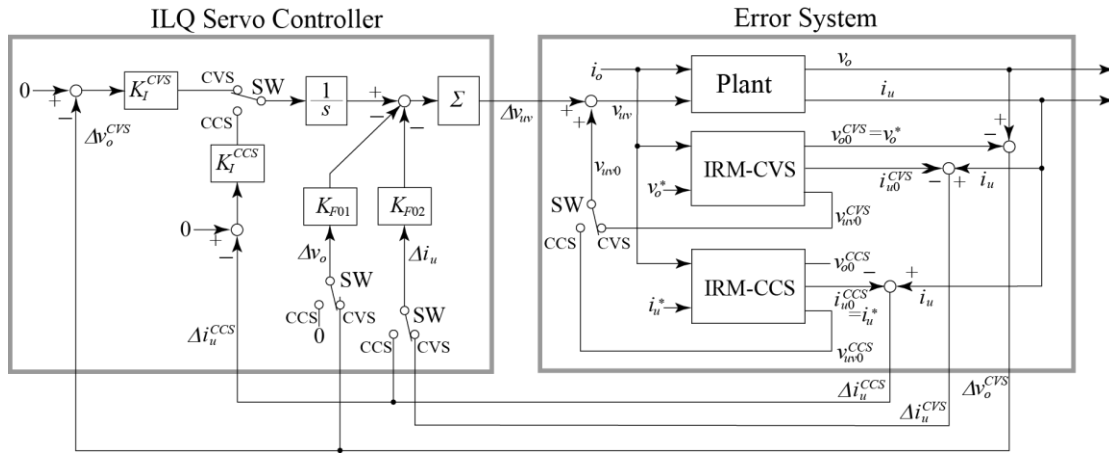


Figure 3. Configuration of the Hybrid Voltage and Current Control System by IRM-ILQ Servo Control.

TABLE I. PARAMETERS OF THE SINGLE-PHASE INVERTER AND GAIN ADJUSTING FOR OPTIMAL CONDITION OF THE ILQ CONTROLLER

Parameters	Values
L_F	0.25mH
r	0.1mΩ
C_F	4.7 μF
R_o	100kΩ

D. Simulation

In the first simulation we are focusing on the resistance and the inductance with frequency $f=1\text{kHz}$, $\omega=2\pi f$. In that experiment we define the load as R (resistance), L (inductance) and C (capacitor) in series. To obtain the values of the parameters we used two formulas such $R=\omega L$ and $f^2=1/4\pi^2 LC$. Fig.4 shown that the curve of the current i_u (red) for $R=7.07\Omega$ and $L=1.125\text{mH}$ follows the command control with small fluctuations. In the second simulation we are focusing on the resistance and capacitor. This time, we used the same resistance $R=7.07\Omega$ and $C=25.511\mu\text{F}$ in Fig.5 and we noticed the same result in the previous simulation but with no fluctuations. In Fig.6 we set -50% error and the output voltage follows the

command control and suppresses the current (current limit). However, for all the simulations, if the current exceeds the upper current limit the CVS will change to CCS to be able to suppress the overcurrent to protect the controller.

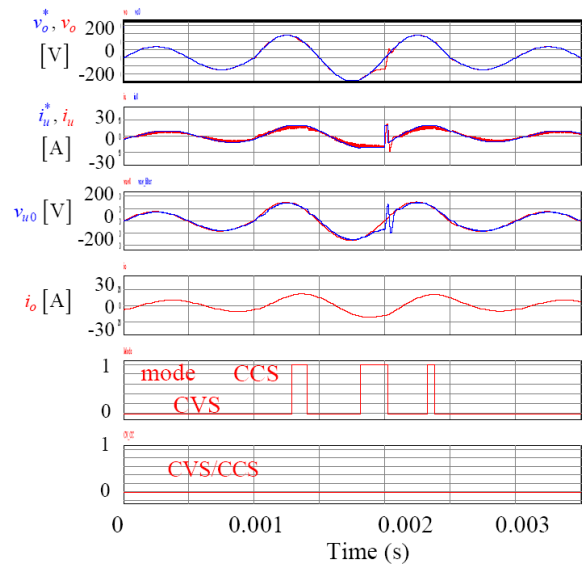


Figure 4. CVS and CCS mode ($R=7.07\Omega$, $L=1.125\text{mH}$, $\text{PF}=0.5\text{lag}$) (Current limit $10\text{A} \pm 3\text{A}$, $50\text{Vrms} \rightarrow 100\text{Vrms} \rightarrow 50\text{Vrms}$).

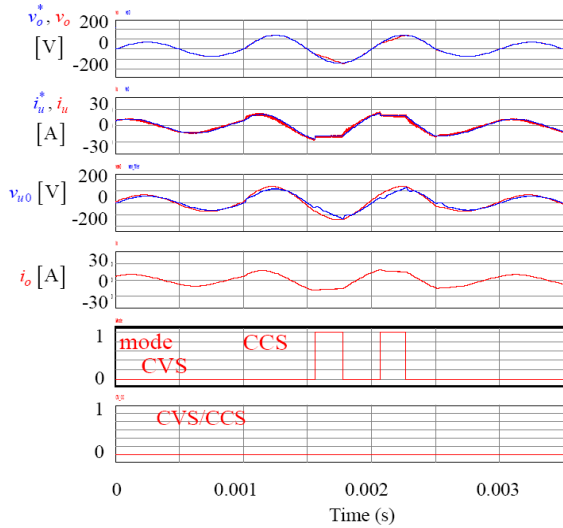


Figure 5. CVS and CCS mode ($R=7.07\Omega$, $C=22.511\mu\text{F}$, $\text{PF}=0.5\text{lead}$) (Current limit $10\text{A}\pm 3\text{A}$, $50\text{Vrms} \rightarrow 100\text{Vrms} \rightarrow 50\text{Vrms}$).

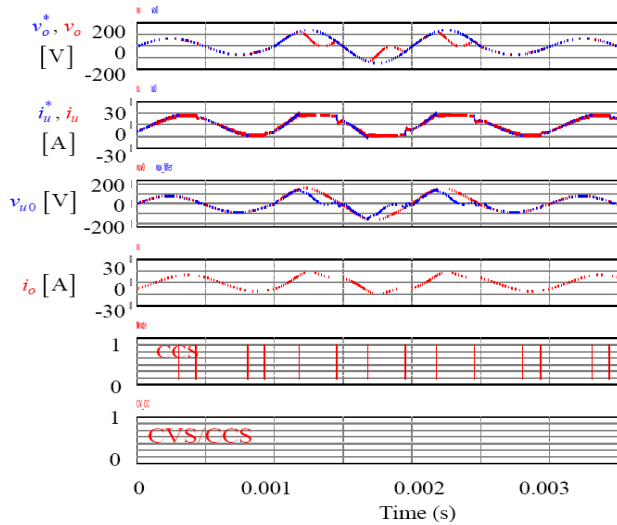


Figure 6. CVS and CCS mode with -50% error ($R=7.07*0.5\Omega$, $C=22.511*0.5\mu\text{F}$, $\text{PF}=0.5\text{lead}$) (Current limit $10\text{A}\pm 3\text{A}$, $50\text{Vrms} \rightarrow 100\text{Vrms} \rightarrow 50\text{Vrms}$).

III. CONCLUSION

In this paper we succeeded to test the robustness evaluation for ILQ optimal control based on inverse reference model (IRM). On CVS mode the actual voltage v_o follows to its command $v_o^* = v_{o0}$. Moreover, in CCS mode actual current i_u follows to its command $i_u^* = i_{u0}$ even if any power factor load including parameter errors. By using PSIM simulator we realized that the CVS can convert to CCS if we reach the upper limit current to protect the controller.

AUTHOR CONTRIBUTIONS

I thank my supervisor FUMINORI ISHIBASHI for his contribution and support such as corrections and figures.

ACKNOWLEDGMENT

I wish to thank Shibaura Institute of technology, JICE and JICA for their support

REFERENCES

- [1] Ministry of Economy, Trade and Industry, Agency for Natural Resources and Energy: "Basic Energy Plan 2014," Economic and Industrial Research Meeting, (2014)
- [2] N. Ichihiro, "Development of Stirling engine resurfaced dream engine," Industrial Research Association, 1982.
- [3] Military Work, Hirohiko Yoneda, "Stirling engine: Its upbringing and principle," Power Co., Ltd., 2009.
- [4] A. Hoshi, Ichinoseki, S. Sato, and K. Maezawa, "Investigation of waste heat recovery and generation system by free piston stirling engine," *The Japan Society of Mechanical Engineers*, pp. 269-272, June 2010.
- [5] Ministry of Economy, Trade and Industry ordinance to amend part of the Ordinance stipulating the rules of the Enforcement of the Electric Ity Act and the Technical Standards for Thermal Power Equipment" on the Ministry of Economy, Trade and Industry website http://www.meti.go.jp/policy/safety_security/industrial_safety/oshirase/2014/11/2601105-1.html, Nov 5, 2014
- [6] H. Ohgami, Revision of the Electricity Business Law on Stirling Engine Power Generation," in *Proc. The 8th Stirling Engine Lecture of the Japan Stirling Engine Promotion Association: Revision of the Electricity Business Law and Stirling Engine Power Generation Business - Proceedings*, pp. 19-35, December 2, 2014.
- [7] K. G. Co., Ltd. And others: "Development of biogas power generation equipment with low-cost small methane fermentation and deodorization function," Kanto Bureau of Economy, Trade and Industry Heisei 23 Strategic Basic Technology Sophistication Support Project Research and Development Results Report, March 2012
- [8] S. Kanda, H. Takami, "Prototype 1kW stirling engine generating system by single-phase boost converter", Annual Meeting of Electrical Engineering of Japan, 4-021, pp. 33-34 (2014-3) (in Japanese)



Ka Ahmadou Master 2 student at shibaura Institute of Technology. I have two bachelors in Senegal, the first bachelor was earned in 2013 In Physics and chemistry at cheikh Anta Diop University of Dakar and the second bachelor I got it in 2017 at Intitute Superior of technology and Industrial in Electro-technic Electromechanic refrigeration and air conditioning.



Hiroshi Takami (Member) received the Ph. D in Electrical Engineering from the Kyushu University in1992. From 1993 to 2005, he was a Research Associate with the Department of Electrical Engineering, Kyushu University. From 2005 to 2008, he was Associate Professor with the Department of Electrical Engineering, Faculty of Engineering, Shibaura Institute of Technology, Tokyo Japan, and since 2008 he has been a Professor. He is engaged in the development of the optimal control for power electric systems and motors, renewal energy generation system including Stirling engine control system. In 2016 he invented a hybrid power supply vehicle combined PV and Stirling engine generator fed by biomass wood pellet. Prof. Dr. Takami is a member of the Institute of Electrical Engineers of Japan, the Society of Instrument and Control Engineers of Japan and the Institute of Electrical and Electronic Engineers of USA (IEEE USA).